

# Non-Equilibrium Thermodynamic Description of the Coupling between Structural and Entropic Modes in Supercooled Liquids

R. Di Leonardo<sup>1</sup>, A. Taschin<sup>2</sup>, M. Sampoli<sup>2,3</sup>, R. Torre<sup>2</sup>, G. Ruocco<sup>1</sup>,

<sup>1</sup>*Dipartimento di Fisica and INFN, Università di Roma "La Sapienza", I-00185, Roma, Italy.*

<sup>2</sup>*Dipartimento di Fisica, LENS and INFN, Università di Firenze, I-50019 Sesto, Firenze, Italy.*

<sup>3</sup>*Dipartimento di Energetica, Università di Firenze, via S. Marta, Firenze, Italy.*

(Dated: November 11, 2018)

The density response of supercooled glycerol to an impulsive stimulated thermal grating ( $q=0.63 \mu\text{m}^{-1}$ ) has been studied in the temperature range ( $T=200\div 340$  K) where the structure rearrangement ( $\alpha$ -relaxation) and thermal diffusion occur on the same time scale. A strong interaction between the two modes occurs giving rise to a dip in the  $T$ -dependence of the apparent thermal conductivity and a flattening of the apparent  $\alpha$ -relaxation time upon cooling. A non-equilibrium thermodynamic (NET) model for the long time response has been developed. The model is capable to reproduce the experimental data and to explain the observed phenomenology.

PACS numbers: 05.70.Ln, 78.47.+p, 64.70.Pf.

Whenever an inhomogeneous temperature or pressure field exists inside a substance, heat and momentum will flow giving rise to processes, like thermal diffusion and sound propagation, which drive the system toward homogeneity. In a normal liquid, at low enough wave-vector  $q$  (i.e. at typical values of light scattering experiments), the time-scales of the two processes are well separated, so that sound propagation is adiabatic and thermal diffusion is isobaric. Every other microscopic process evolves on such a fast time-scale that it enters the dynamic equations simply by determining the actual values of thermodynamic derivatives and transport coefficients. The situation changes when a liquid is supercooled below its melting temperature and the structural relaxation time,  $\tau_\alpha$ , rapidly grows up upon cooling. When  $\tau_\alpha$  becomes of the order of magnitude of the sound wave period, we observe phenomena as the sound velocity dispersion and sound absorption. These phenomena have been widely investigated by ultrasonic and Brillouin spectroscopies and commonly described in terms of a relaxing bulk modulus or viscosity [1, 2]. Upon further cooling,  $\tau_\alpha$  reaches the time scale of the thermal diffusion giving rise to a complex frequency dependent heat diffusion that is observed experimentally by specific heat spectroscopy [3] and forced Rayleigh scattering [4, 5]. Though both viscosity and specific heat relaxations are manifestation of the same microscopic process, there is no commonly accepted formulation of the dynamic equations in the region where structural relaxation and thermal diffusion occur on the same time-scale. The main difficulty arises when more than one single thermodynamic derivative has to be generalized to have a frequency dependence. To this respect NET provides a more fundamental approach, compared to generalized hydrodynamics, since, once the equation of state is properly written in a suitable extended parameter space, the frequency dependence of generalized thermodynamic derivatives comes out naturally. Moreover a thermodynamic approach could, hopefully, be related to that thermodynamic picture of supercooled and glassy state which has recently been the

subject of great theoretical and computational efforts [6]. Unfortunately whether local thermodynamic equilibrium is still meaningful in the supercooled regime and what are the crucial steps in extending the thermodynamic parameters space are still open questions.

In this work we present an Impulsive Stimulated Thermal Scattering (ISTS) [7] study of liquid and supercooled glycerol in a temperature range that covers the region where the characteristic times of structural and entropic modes become similar. A strong interaction between the two modes occurs and we have observed an apparent slow down of the steep increase of structural relaxation upon cooling, together with a marked non exponential decay at long times where the ISTS signal is usually governed by thermal diffusion. The NET model we propose is based on local thermodynamic equilibrium in an extended parameter space [8]. Using literature data, we reproduced accurately the experimental ISTS responses at long times and explained unexpected features such as the dip in the  $T$ -dependence of the thermal conductivity of various supercooled liquids [4, 5, 9].

Glycerol (99.5+%, <0.1% water, Fluka, glass transition temperature 185 K) was transferred under nitrogen into a Teflon-coated cell with movable windows [10]. The cell was mounted on the cold finger of a cryostat and outfitted with resistive heaters. A platinum resistance thermometer was immersed in the sample and the temperature was kept stable within  $\pm 0.1$  K. In the present ISTS experiment two infrared ( $\lambda = 1064$  nm) short ( $\sim 100$  ps) laser pulses cross each other in the sample volume at an angle of  $\sim 6^\circ$  ( $q = 0.63 \mu\text{m}^{-1}$ ) and their interference produces an impulsive, spatially modulated, heating. The amplitude of the resulting density grating is probed by a third CW laser beam ( $\lambda = 532$  nm) impinging on the induced grating at the Bragg angle. The intensity of the diffracted beam as a function of time is stored by a digital oscilloscope and averaged over many ( $\approx 5000$ ) pulses. The measured signal can be fully ascribed to density dynamics excited through heating since electrostrictive and birefringence effects are negligible in

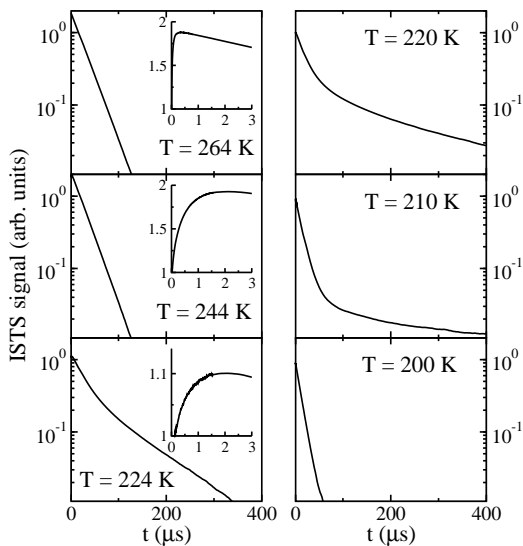


FIG. 1: ISTS data of supercooled glycerol at selected temperatures are reported in logarithmic scale and normalized to unity at about  $t = 0.1\mu\text{s}$ . The inserts show a blow up of the short time region, where the structural relaxation gives rise to a rising signal.

glycerol [11, 12, 13]. Further experimental details are reported in Ref. [9]. ISTS data were collected in the temperature range  $T=200\div 340$  K. Signals as long as 1.6 ms were recorded with a time resolution of 1 ns. In the present paper we focus on the long time part of ISTS signal ( $t > 0.1\mu\text{s}$ ) where the acoustic transient is over and structural and entropy modes evolve isobarically. Selected ISTS data are reported in Fig. 1 showing two time regions: “short times” ( $t < 10\mu\text{s}$ ) in the inserts and longer times in the main panels. It can be noted that at short times the amplitude of the density grating (ISTS signal) increases with a stretched exponential law, due to structural relaxation. On lowering the temperature, the characteristic time of this rising component stops to grow while its intensity vanishes. At longer times the heat diffuses and the density grating decays to zero. This long time decay, which in absence of coupling is exponential (due to the diffusive character of heat equation) [7], now splits into two components. The faster component is nearly exponential and its time constant goes through a maximum and gives rise to a dip in the apparent thermal diffusivity, as already reported for OTP in [9]. The slower component shows a strong non-exponentiality. It flattens out and its intensity disappears as the temperature is lowered. To be more quantitative, we fitted the data with two stretched exponentials for the “structural” rising component and the long time tail, and a simple exponential for the intermediate time component (apparent thermal diffusion). The decay rates [14] of the short and intermediate components are reported in Fig. 2. At high temperatures, the structural relaxation decay rate ( $\circ$ ) is described by a Vogel-Tamman-Fulcher (VTF) law (full line). The parameters  $B=2260$  K,  $T_{VTF}=131$  K of VTF

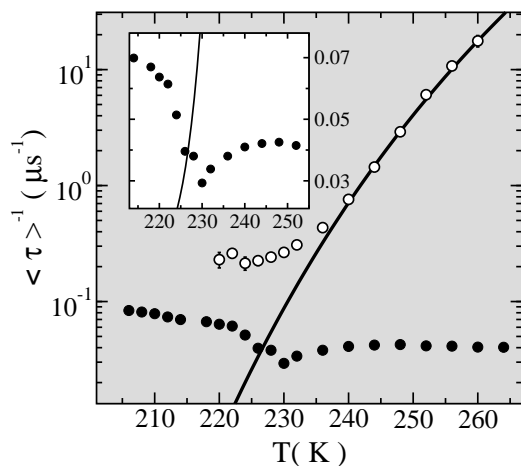


FIG. 2: Temperature dependence of characteristic rates for the short rising component -apparent structural relaxation- ( $\circ$ ) and intermediate exponential decay -apparent thermal diffusion- ( $\bullet$ ). Solid line is the VTF law  $\gamma_{VTF} = \tau_0^{-1} \exp[-2260K/(T - 131K)]$

law,  $\gamma_{VTF} = \tau_0^{-1} \exp[-B/(T - T_{VTF})]$  are taken from dielectric spectroscopy [15] while  $\tau_0 = 1.4 \cdot 10^{-15}\text{s}$  is scaled to fit the data. At temperatures lower than  $\sim 240$  K the short time rising component ceases to represent the structural relaxation and flattens around a value of  $4\mu\text{s}$ . At about the same temperature, the apparent thermal decay rate deviates from the expected smooth behavior (see the insert of Fig. 2) and exhibits a dip at  $T \approx 230$  K. The overall scenario depicted in Fig. 2 suggests the existence of an interaction between the structural and thermal relaxation dynamics that leads to a complex relaxation time pattern. In the following we will introduce a NET model that will allow us to compute the temperature evolution of this relaxation times pattern and find a very good agreement with the experimental observations. NET [8] provides a very powerful framework to study irreversible processes such as heat conduction, diffusion and viscous flow, from a unified point of view. However, in this formalism, it is not straightforward to consider the non-exponentiality observed in the structural relaxation dynamics. On the contrary, the presence of a large number of internal relaxing variables can be easily taken into account provided that local thermodynamic equilibrium is valid in the extended parameter space. Therefore, following Allain et al.[16], we choose to represent the observed non-exponentiality as the result of the superposition of  $N$  linearly relaxing variables [17]. In this hypothesis the Gibbs free energy law per unit mass reads:

$$dg = vdp - sdT - \sum_{i=1}^N A^i d\xi^i \quad (1)$$

where  $p$  is the pressure,  $s$  the entropy,  $A^i$  the affinity of the  $i^{\text{th}}$  relaxation process and  $\xi^i$  the correspondent progress variable (or order parameter). As noted above, we are interested in the time region where the pressure became and stays uniform. In this time region,

the linearized NET equations[8] written in terms of the q-components of the thermodynamic variables (e.g.  $T$  stands for  $T(t) = \int \exp(i\mathbf{q}\mathbf{r})T(\mathbf{r}, t)$ ), are:

$$\begin{aligned} p &= 0 \\ T_0\rho_0(\partial s/\partial t) &= -q^2\lambda T \\ \partial\xi^i/\partial t &= -\beta^i A^i \end{aligned} \quad (2)$$

where  $T_0$  ( $\rho_0$ ) is the average temperature (density),  $\lambda$  the thermal conductivity and  $\beta^i$  phenomenologic constants. The first of (2) comes from the linearized combined mass momentum conservation laws [19]. The second and third equations of (2) represent the energy conservation law and the phenomenological relations for the relaxation processes respectively. In order to close the above set of equations, we use the local thermal equilibrium in the extended parameter space:

$$\begin{aligned} \rho &= \rho(p, T, \xi^1, \dots, \xi^N) \\ s &= s(p, T, \xi^1, \dots, \xi^N) \\ A^i &= A^i(p, T, \xi^i) \end{aligned} \quad (3)$$

For simplicity, we assume that the thermodynamic affinity  $A^i$  does not depend on  $\xi^j$  for  $j \neq i$ . Differentiating the above equations and substituting in (2) we obtain:

$$\rho = -\rho_0\alpha^\infty T + (\rho_0^2 c_p^\infty / T_0) \sum_{i=1}^N \Delta^i (\xi_p^i / \xi_T^i) \zeta^i \quad (4)$$

$$\partial T / \partial t = -\Gamma_H^\infty T - \sum_{i=1}^N \Gamma_R^i \Delta^i (T - \zeta^i) \quad (5)$$

$$\partial \zeta^i / \partial t = -\Gamma_R^i (\zeta^i - T) \quad (6)$$

where we have introduced the following symbols:

$$\begin{aligned} \alpha^\infty &= -\rho^{-1} (\partial \rho / \partial T)_{p\xi} & c_p^\infty &= T_0 (\partial S / \partial T)_{p\xi} \\ \Delta^i &= T_0 A_\xi^i \xi_T^{i2} / c_p^\infty & A_\xi^i &= (\partial A^i / \partial \xi^i)_{pT} \\ \xi_p^i &= (\partial \xi^i / \partial p)_{A^i T} & \xi_T^i &= (\partial \xi^i / \partial T)_{A^i p} \\ \zeta^i &= \xi^i / \xi_T^i & \Gamma_H^\infty &= \lambda q^2 / \rho_0 c_p^\infty \end{aligned} \quad (7)$$

The ISTS density response is obtained by solving (5,6) for the initial condition  $T(0) \neq 0$ ,  $\xi^i(0)=0$  and then substituting in (4). To reduce the number of parameters, we use the simplifying assumption that  $\xi_p^i / \xi_T^i$  is independent of  $i$  [16]. In that case,  $\rho(t)$  can be written as

$$\rho(t) / \rho(0) = -T(t) / T(0) - \frac{\Delta\alpha}{\alpha^\infty} \frac{c_p^\infty}{\Delta c_p} \sum_{i=1}^N \Delta^i \zeta^i(t) \quad (8)$$

where  $\Delta\alpha$  and  $\Delta c_p$  are the jump from the relaxed to the unrelaxed (with respect to the  $\zeta^i$ ) values of the corresponding thermodynamic derivatives. It can be easily shown that in the limit  $\Gamma_R^i \ll \Gamma_H^\infty$  - i.e. at low T or high q values- this model predicts a density-density correlation function which at long times decays as:

$$\phi_q(t) \propto \sum_{i=1}^N \Delta^i \exp[-\Gamma_R^i t] \quad (9)$$

We know from photocorrelation experiments, Mode Coupling Theory and molecular dynamics simulations, that the above correlator is very well described by a stretched

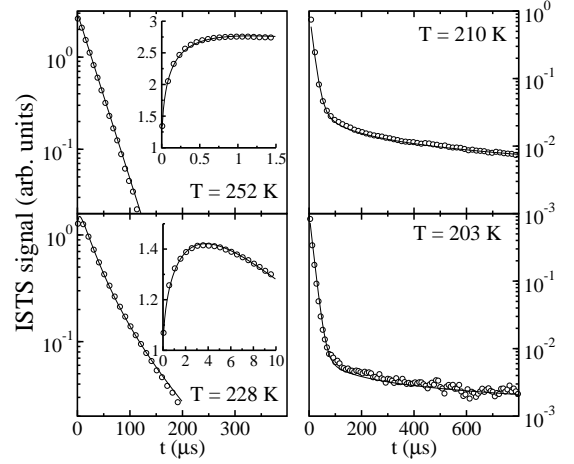


FIG. 3: ISTS data ( $\circ$ ) and the predicted signal (solid line) for four different temperatures. The agreement is very good through the whole structural-entropic coupling region

exponential  $\exp[-(t/\tau_\alpha)^\beta]$  where  $\beta$  is slightly changing with temperature and  $\tau_\alpha$  obeys a VTF law. Relying on this considerations, we arbitrarily choose a distribution of  $N=150$  [20] logarithmically spaced rates  $\Gamma_R^i = (\Gamma_\alpha) 10^{x_i}$ ,  $x_i = -1 + i/28$ , with weights  $\Delta^i$  such that the sum (9) reconstructs a stretched exponential with  $\beta=0.65$  [3, 11]. This determines the weights apart from a constant factor which in turn can be easily fixed by the value of  $\Delta c_p / c_p^\infty = \sum \Delta^i$  from specific heat spectroscopy data[3]. The temperature simply changes the value of  $\Gamma_\alpha$  which is assumed to obey the already quoted VTF law. We can assume  $\Gamma_H^\infty(T) = (c_p^0 / c_p^\infty) \Gamma_H^0(T)$  where  $\Gamma_H^0(T)$  is the extrapolation to the whole temperature range of ISTS thermal decay rates at high temperature. Finally, from  $\rho(T)$  data across the glass transition temperature [21] one finds  $\Delta\alpha \sim 3.2\alpha^\infty$ . We are now left with no more free parameters: for each temperature we can compute the ISTS signal and compare it to the experimental data. As examples, the results of this comparison are shown in Fig. 3 for four different temperatures, showing an excellent good agreement between the data ( $\circ$ ) and the model (solid line) in the whole examined temperature range. A complementary and more insightful way of representing complex time responses consists in performing an inverse Laplace transform analysis:  $I(t) = \int_{-\infty}^{\infty} G(\log \gamma) \exp[-\gamma t] d \log \gamma$ . In other words, one can think of the ISTS signal as a superposition of exponentials and ask how the weight function  $G$  evolves across the coupling region. In this representation it is easier to visualize the analyzed phenomenology as the interaction between an exponential thermal process and a broad distribution of relaxing variables. As a consequence, the relation between the flattening in the "structural" rate, the dip in the thermal rate and the appearance of a long time tail becomes evident. Such an analysis has been carried out on the simulated signals and is summarized in Figs. 4. The top figure in the right panel represents  $G$  in the high temperature region

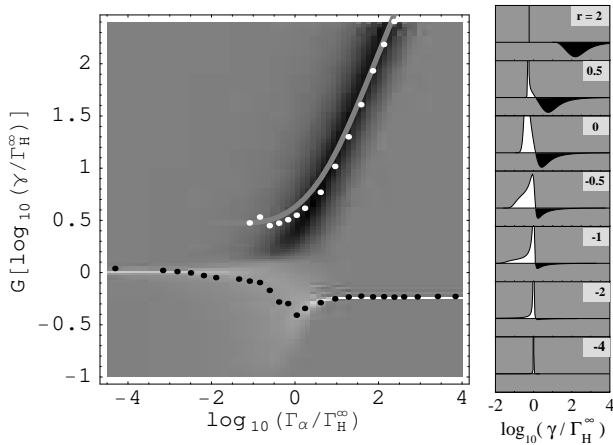


FIG. 4: Computed evolution of the distribution of rates  $G$  as a function of the logarithmic ratio  $r = \log_{10}(\Gamma_\alpha/\Gamma_H^\infty)$  between structural relaxation characteristic rate and the infinite frequency thermal decay rate. Circles in the left panel represent the experimental values

where no coupling is present. Structural relaxation manifests itself as a rising (negative weight) stretched (broad distribution) exponential, while at longer times (smaller rates) thermal diffusion contributes to the signal with an exponentially (narrow) decaying (positive weight) component. As the temperature is lowered, the broad structural mode moves to shorter rates until the tail of its rate

distribution reaches the entropy mode time scale. As a result, the time scale of the negative component ceases to vary and its intensity vanishes. On the other hand, the positive component broadens moving to smaller rates and then splits into two components: a narrow one which moves to larger rates, lowering the temperature, and a broad one which becomes flatter and flatter and decays to zero. In the left panel of Fig. 4, we report the evolution of  $G$  as a function of  $\log_{10}(\Gamma_\alpha/\Gamma_H^\infty)$ . Black and white regions represent negative and positive weights respectively. The circles represent the normalized average rates for the rising (white) and first part of decaying (black) portion of the experimental ISTS signal. The solid upper line is the computed inverse average time  $1/\langle \tau \rangle$  of the negative component.

In conclusion, a NET model, based on the assumption of local thermodynamic equilibrium in an extended parameter space, accounts for the rich phenomenology observed in the ISTS experiments. In particular, using new ISTS data on supercooled glycerol in the temperature region where the structural relaxation and the thermal diffusion process take place on the same time scale, we have demonstrated that the model is able to reproduce the experimental data using literature data from other experiments. Further investigations on the possibility of assuming local thermodynamic equilibrium in supercooled liquids are crucial in the development of a thermodynamic description of glass-forming liquids. This work was supported by INFN, MURST and EC grant N. HPRI-CT1999-00111.

- 
- [1] R.D. Mountain, *Rev. Mod. Phys.*, **38**, 205, (1968).  
[2] R. Zwanzig, *J. Chem. Phys.*, **43**, 714, (1965).  
[3] N.O. Birge *Phys. Rev. B*, **34**, 1631, (1986).  
[4] C. Allain and P. Lallemand, *J. Phys. (Paris)*, **40**, 693 (1979).  
[5] W. Köhler, G. Fytas, W. Steffen and L. Reinhardt, *J. Chem. Phys.*, **104**, 248, (1996).  
[6] E. La Nave, S. Mossa and F. Sciortino, *Phys. Rev. Lett.* **88**, 225701 (2002); Th.M. Nieuwenhuizen, *Phys. Rev. Lett.* **80**, 5580-5583 (1998).  
[7] Y. Yang and K. Nelson, *J. Chem. Phys.* **103**, 7722 (1995); **103**, 7732 (1995).  
[8] S.R. de Groot and P. Mazur, *Non Equilibrium Thermodynamics*, Dover Editions (1962).  
[9] R. Torre, A. Taschin, and M. Sampoli, *Phys. Rev. E*, **64**, 61504, (2001).  
[10] I. Halalay, K. Nelson, *Rev. Sci. Instrum.* **61**, 3623 (1990).  
[11] D.M. Paolucci and K. Nelson, *J. Chem. Phys.* **112**, 6725, (2000).  
[12] A. Taschin, R. Torre, M. Ricci, M. Sampoli, C. Dreyfus and R.M. Pick, *Europhys. Lett.*, **53**, 407, (2001).  
[13] C. Glorieux, K.A. Nelson, G. Hinze and M.D. Fayer, *J. Chem. Phys.*, **110**, 3384, (2002).  
[14] Inverse average time  $\langle \tau \rangle^{-1} = \gamma\beta/\Gamma(1/\beta)$  is used as characteristic rate of the stretched exponential.  
[15] P. Lunkenheimer et al., *Europhys. Lett.* **33**, 611 (1995).  
[16] C. Allain, P. Lallemand, and N. Ostrowsky, *Mol. Phys.*, **31**, 581 (1976); C. Allain and P. Lallemand, *J. Phys. (Paris)*, **48**, 679 (1979).  
[17] The number  $N$  should not be read as a number of well defined physical variables, but rather as the discrete representation of either a distribution of independent debye relaxing variables, or a single strongly non exponential relaxing variable. It is important to note that the specific studies and experiments presented in this work do not allow to find whether the underlying relaxation process is homogeneous and intrinsically non exponential or it is heterogeneous, i.e. the superposition of different, spatially separated, genuine Debye processes (see [18] for a comprehensive review on the subject).  
[18] R. Richert, *J. Phys.: Condens. Matter*, **14**, R703.  
[19]  $\partial^2 \rho / \partial t^2 + (\eta q^2 / \rho_0) \partial \rho / \partial t + q^2 p = 0$ . After the acoustic transient the terms involving derivatives of density are negligible.  
[20] Given the constraints in the model the number of input parameters does not change with  $N$ . We remark that, for  $N$  large enough ( $> 10$ ), the solution is practically independent of  $N$ .  
[21] A.R. Ubbelohde, *Melting and Crystal Structure* (Clarendon, Oxford, 1965).  
[22] C. Demoulin, C.J. Montrose and N. Ostrowsky, *Phys. Rev. A*, **9**, 1740, (1974).